

THE PARTIAL OXIDATION OF METHANOL BY MoO₃(010) SURFACES WITH CONTROLLED DEFECT DISTRIBUTIONS

RICHARD L. SMITH and GREGORY S. ROHRER

Carnegie Mellon University,
Department of Materials Science and Engineering
Pittsburgh, Pennsylvania 15213-3890

ABSTRACT

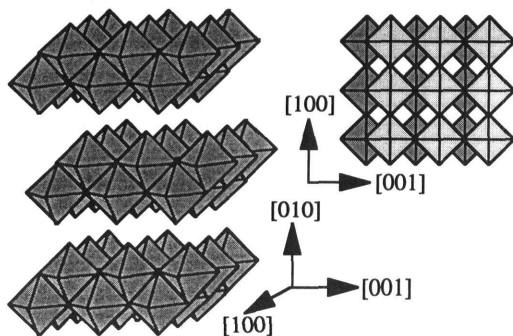
Atomic force microscopy has been used to determine how MoO₃(010) surfaces with controlled defect populations evolve during reactions with MeOH/N₂ mixtures. The structural evolution of the freshly cleaved surface is compared to surfaces reduced in 10% H₂/N₂ at 400 °C. While the freshly cleaved surfaces are flat and nearly ideal, the reduced surfaces contain voids bounded by step loops where Mo atoms in reduced coordination are found. In both cases, reacting the MoO₃(010) surface with MeOH/N₂ mixtures between 300 and 400 °C leads to H intercalation and the nucleation of acicular precipitates of H_xMoO₃. On the freshly cleaved surface, the H-bronze phase precipitates uniformly. On the reduced surface, the precipitates form preferentially at the void edges, where undercoordinated Mo atoms are found.

INTRODUCTION

Molybdenum trioxide (MoO₃) is a common component of catalysts used for the partial oxidation of hydrocarbons. Multi-component materials of practical importance include the Bi-Mo-O catalyst used for propene oxidation and ammoxidation and the Fe-Mo-O catalyst used for the partial oxidation of methanol to formaldehyde. MoO₃ itself has been the focus of many experimental investigations, particularly because many reactions catalyzed by the oxide are thought to be surface-structure sensitive [1-4]. It has been proposed that unsaturated surface sites, where Mo atoms have fewer than six nearest neighbors, are preferential reaction sites for alcohol oxidation [3]. The objective of the experiments described in this paper was to test this idea by intentionally introducing a well-characterized population of undercoordinated Mo on the MoO₃(010) surface and directly observing the morphological evolution during reactions with alcohols.

MoO₃ has the layered structure illustrated in Fig. 1. Each layer is composed of two corner-sharing octahedral nets that link by sharing edges along [001]. Adjacent layers along [010] are linked only by weak van der Waals forces and, when cleaved at the gap between these layers, two identical O-terminated surfaces are created. While the Mo atoms in the ideal surface layer retain their bulk coordination, Mo atoms in alternative coordinations exist at step edges. If a step is created along [001] by breaking Mo-O-Mo linkages, one half of the metal atoms are left in a five-coordinate site. If, on the other hand, a step is created along [100], two Mo-O-Mo linkages are

Figure 1. Polyhedral representation of the MoO₃ structure. MoO₃ has a primitive orthorhombic cell (Pbnm) and its lattice parameters are a=3.963 Å, b=13.856 Å, c=3.6966 Å.



broken for each Mo atom and the average Mo coordination number along the step must be 5. In this case, the average might be made up of equal numbers of 4- and 6-coordinate Mo.

Experimentally, it is possible to produce undercoordinated sites with reducing treatments at 400 °C in H₂/N₂ mixtures [5]. Under these conditions, voids, bounded by step loops, form on the surface. We have used atomic force microscopy (AFM) to characterize both the freshly cleaved surface and surfaces containing voids. In this paper, we describe the evolution of these two characteristic surfaces during reactions in MeOH/N₂ mixtures. In each case, H_xMoO₃ precipitates are observed to form as a product of the reaction, but the distribution of the precipitates differs. The mechanisms by which the undercoordinated Mo at the edges of the voids might affect the transfer of protons from the alcohol to MoO₃ are discussed.

EXPERIMENTAL

Single crystals of MoO₃ were grown by chemical vapor transport in sealed, evacuated quartz ampoules [6]. The surface reactions were performed in a quartz tube with flowing gas at 1 atm. A magnetic transfer rod (consisting of a permanent magnet sealed within a quartz rod) was used to move the samples into and out of the hot zone of the furnace. The single crystals were mounted on a steel disc by spot welding a thin strip of Ta foil across the basal facet. The steel disc was attached to the transfer rod by chromel wire spring clips. After cleaving the crystal and sealing the reaction tube, the system was purged by alternately evacuating and backfilling with the reactant gas mixture three times. The samples were then transferred to the hot zone of the furnace and reacted for a pre-determined time at temperature.

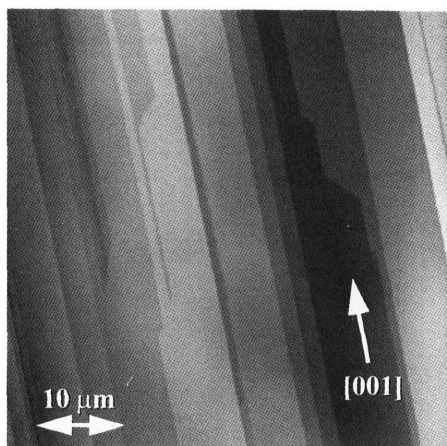
To create surface voids with undercoordinated Mo atoms, as-received 10%H₂/N₂ (forming gas) with a nominal H₂O concentration of 20 ppm was used to reduce the samples at 400°C in a 350 cc/min flow of the gas. Samples were then transferred to the cool zone of the reaction tube and allowed to sit under a flow of forming gas for approximately 30 min while the hot zone was cooled to the desired temperature for the MeOH reaction. Subsequently, the gas composition was changed to a MeOH/N₂ mixture and the sample was transferred back to the hot zone for reaction under a 200 cc/min flow. The N₂ (Prepurified, Matheson) carrier gas was dried with CaSO₄ (Drierite) and a liquid N₂ trap prior to being saturated in a methanol (99.9+%, Aldrich) bubbler. Following reaction, the MoO₃ samples were cooled to room temperature under a flow of the reactant gas mixture and then transferred to an AFM housed in a glove box with an atmosphere of continuously-purified Ar (O₂ and H₂O < 5 ppm). In most cases, the samples were transferred directly to the glove box without exposing them to the ambient atmosphere. However, the microstructural changes observed on surfaces which were momentarily exposed to the ambient did not differ from those of samples which were not exposed to air.

X-ray diffraction (XRD) was used to identify the phase that formed on the MoO₃(010) surfaces during the reactions with methanol. First, a number of crystals were reacted simultaneously in a silica boat. To selectively probe the near surface region, the reacted (010) surface layers (thickness < 20 μm) were cleaved from the crystals with adhesive tape, pulverized, and immediately subjected to XRD analysis. The small quantity of powder obtained with this procedure was mounted on a glass slide covered with a layer of double-sided tape. At least one of the crystals from each batch was characterized with AFM to ensure that the surface structure could be directly correlated with the X-ray data. In some cases, parallel experiments with powders were also performed. All X-ray data were recorded in the ambient on a Rigaku Θ-2Θ diffractometer with Cu K_α radiation. Lattice parameters were refined using a least squares method.

RESULTS

The freshly cleaved (010) surface is characterized by atomically flat terraces separated by steps whose heights are always an integer multiple of 7 Å (7 Å ≈ b/2). Steps with heights greater than 28 Å (2 unit cells) are rarely observed. The step edges are almost exclusively oriented along the [001] axis of the crystal, as can be seen in the characteristic AFM image in Fig. 2. Creation of steps of this orientation requires the minimum number of broken bonds per unit length of step.

Figure 2. Contact AFM image of the cleaved $\text{MoO}_3(010)$ surface. Characteristically, surface steps run parallel to $[001]$ and step heights are always an integer multiple of 7 \AA ($b/2$).



Reactions with MeOH/N_2 mixtures between 300 and $340 \text{ }^\circ\text{C}$ lead to easily observed changes in the surface structure. Within 10 min of reaction at $330 \text{ }^\circ\text{C}$, the surface is decorated with a cross hatched pattern of acicular precipitates oriented along $\langle 203 \rangle$ (see Fig. 3a). The precipitates continue to grow with increasing reaction times and after extended reactions ($t = 20$ min), they coalesce and assume a second habit parallel to $[001]$ (see Fig. 3b). These structures along $[001]$ are very straight and can have lengths up to several millimeters. The precipitates appear white in AFM images because they rise out of the MoO_3 matrix.

Powder XRD experiments unambiguously identified the $\langle 203 \rangle$ precipitates. The powder XRD patterns from reacted surface layers with microstructures similar to the one shown in Fig. 3b clearly show that the surface is composed of a two phase mixture. In Fig. 4, a portion of a representative pattern is compared to that of unreacted MoO_3 so that the peaks from the second phase can be easily identified. The new peaks in the XRD pattern of the reacted material, which we associate with the $\langle 203 \rangle$ precipitates, can be indexed to a C-centered orthorhombic cell

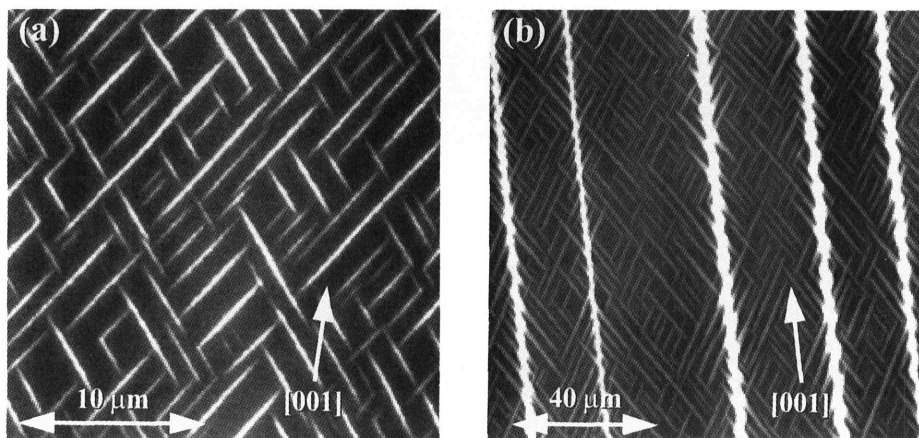


Figure 3. Contact AFM images of $\text{MoO}_3(010)$ surfaces after reaction with N_2 saturated with MeOH ($25 \text{ }^\circ\text{C}$) for (a) 8 and (b) 20 min. at $330 \text{ }^\circ\text{C}$. The black-to-white contrast is (a) 50 \AA and (b) 500 \AA .

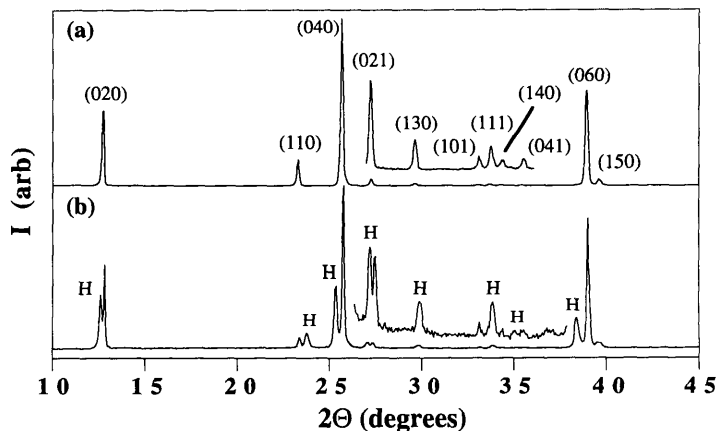


Figure 4. (a) Powder XRD pattern of pure MoO_3 . (b) Powder XRD pattern of pulverized surface layers cleaved from MoO_3 single crystals reacted for 10 min. at 400°C in MeOH/N_2 . Peaks associated with the $\langle 203 \rangle$ precipitates are labeled with an H.

(Cmcm) with refined lattice parameters ($a = 3.8830$ (9), $b = 14.0538$ (25), $c = 3.7282$ (16)) identical to those of the hydrogen bronze phase, H_xMoO_3 , where $0.23 \leq x \leq 0.4$ [7]. Every peak in the XRD pattern can be indexed to either MoO_3 or H_xMoO_3 . The XRD peak positions from surface layers and powders reacted between 300°C and 350°C are identical. Furthermore, patterns from layers with the long $[001]$ features (as in Fig. 3b) indicate that these features are the same H_xMoO_3 phase. These results are consistent with earlier XRD studies which showed that H_xMoO_3 forms during reactions between MoO_3 powder and MeOH/N_2 mixtures at 200°C [8,9]. A more complete description of H_xMoO_3 formation in MoO_3 is found in Ref. [10].

When the (010) surface is reduced in $10\%\text{H}_2/\text{N}_2$ at 400°C , it is modified in two ways. First, crystallographic shear (CS) planes nucleate along the $[001]$ axis of the crystal within 1 min of reduction [11-14]. In AFM images, the CS planes appear as straight, 1.5 \AA surface steps [5] that form to accommodate oxygen deficiency brought on by the reducing treatment. The second modification is the nucleation of voids on the (010) surface planes (see Fig. 5). Voids nucleate within about 5 min and are initially small, with diameters less than 500 \AA and depths on the order of 50 \AA . The voids are bounded by step loops that must have Mo atoms in reduced coordination. With increasing reaction times, the voids grow in depth and breadth and their edges show a preferred orientation, nearly parallel to $\langle 101 \rangle$. It has been demonstrated that water vapor, present as an impurity or a reaction product, catalyzes void formation and growth [5]. Structural modifications were not detected with AFM on surfaces reduced below 350°C .

When MoO_3 samples are reduced in $10\%\text{H}_2/\text{N}_2$ at 400°C before being reacted in MeOH/N_2 at 330°C , the (010) surface is modified in much the same way as the freshly cleaved surface; acicular precipitates of H_xMoO_3 nucleate along $\langle 203 \rangle$. However, the precipitation reaction is favored at the voids. After 2 min at 330°C in MeOH , H_xMoO_3 precipitates are typically found in the vicinity of voids (see Fig. 6a). In the image, an H_xMoO_3 precipitate can clearly be seen emerging from the void labeled with a "V". Additional defects with a distinct $[001]$ character have also formed near the voids. These features appear to be similar to defects observed at higher temperatures (400°C) during reactions with MeOH [10] and they are distinguished from the surface/CS plane intersections because the height over the defects is typically much greater (up to 20 \AA) than those observed over the CS planes. In most instances, these features coincide with a CS plane, but they are only as long as the width (along $[001]$) of the void to which they are adjacent. If one follows a CS plane along $[001]$, the height over the CS plane is only 1.5 \AA , but adjacent to voids, the height may be increased to more than 10 \AA . This swelling is not seen on

Figure 5. AFM topograph of an $\text{MoO}_3(010)$ surface which was reduced in $10\% \text{H}_2/\text{N}_2$ for 8 min at 400°C . The black-to-white contrast in this image is 50 \AA .

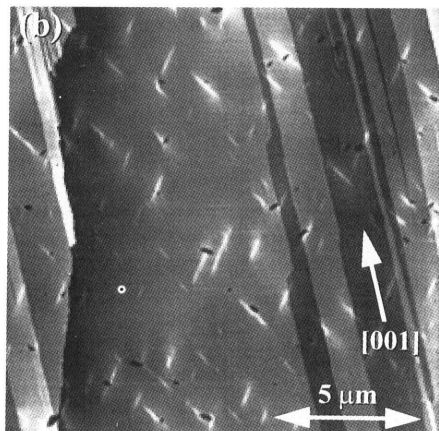
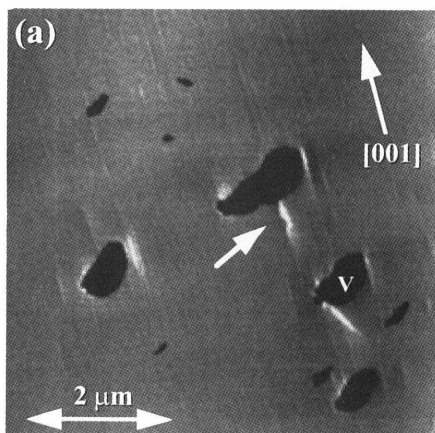
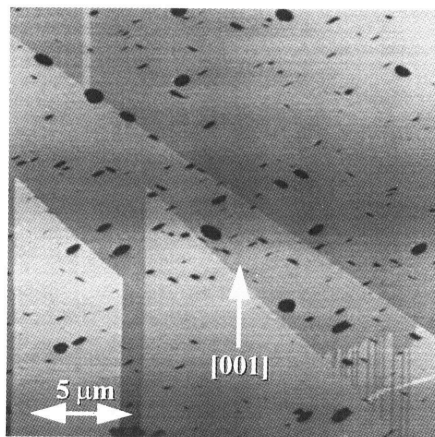


Figure 6. AFM topographs of $\text{MoO}_3(010)$ surfaces reduced in $10\% \text{H}_2/\text{N}_2$ at 400°C for (a) 8 and (b) 4 min and then reacted at 330°C in N_2 saturated with MeOH (0°C) for (a) 2 and (b) 15 min. The black to white contrast in (a) is 20 \AA and in (b) it is 40 \AA .

surfaces which have only been reduced in $10\% \text{H}_2/\text{N}_2$. Finally, note that the feature indicated by the arrow in Fig. 6a shows both $[001]$ and $\langle 203 \rangle$ character.

The preferential nucleation of H_xMoO_3 in the vicinity of the voids is more pronounced with longer reaction times. The H_xMoO_3 precipitates in Fig. 6b are clustered around the voids introduced during reduction. In most cases, the largest precipitates intersect a void and the void-free areas are often without precipitates. In other cases, the precipitates originate at one of the swollen $[001]$ defects adjacent to the void. Finally, we note that similar behavior is observed when the MeOH reaction is carried out within the temperature range between 300 and 400°C .

DISCUSSION AND CONCLUDING REMARKS

When a MeOH molecule is oxidized by MoO₃, two H are abstracted from the alcohol. According to the accepted model, the first is removed during the initial dissociative chemisorption of MeOH and the second is liberated when the surface methoxy decomposes to formaldehyde [15]. While it is usually assumed that the H react with lattice O to form H₂O, under the experimental conditions described here (in the absence of O₂), some fraction of the liberated H intercalates into the MoO₃ structure. Machiels and Sleight [16] observed that in the absence of O₂, the products formed by the reaction of MeOH and MoO₃ included dimethyl ether, hydrogen, and methane, but not formaldehyde. Therefore, methanol chemisorption still occurs in the absence of O₂, but the methoxy species are not further dehydrogenated. This suggests that the intercalating H are produced during the first step of the reaction [10].

The results presented here demonstrate that during methanol oxidation, H_xMoO₃ precipitates form preferentially at the step loops which surround the surface voids. While similar step sites are inevitably found on freshly cleaved surfaces, they have no apparent effect on the intercalation process. This is probably due to the fact that the steps on cleavage surfaces typically have single bilayer heights (7 Å) while the step loops found on pre-reduced surfaces are many times this height. There are two possible explanations for preferential formation of the H_xMoO₃ precipitates in the vicinity of the voids introduced during reduction. The first is that the voids simply act as preferential nucleation sites for H_xMoO₃. In this scenario, H enters the crystal at as yet unidentified surface sites, diffuses to the voids and, finally, precipitates heterogeneously as H_xMoO₃. The second possibility is that H actually intercalates at the void after being removed from the MeOH molecule. The voids not only provide easy steric access to the van der Waals gaps within which the H resides in the H_xMoO₃ structure, but they are also lined with Mo atoms in reduced states of coordination. Such sites have previously been linked to higher activity for the dissociative chemisorption of methanol [2]. Assuming this to be true, then we conclude that MeOH dissociatively chemisorbs at sites on the edges of the voids and as the concentration of dissolved H in the vicinity of the void increases, the H_xMoO₃ precipitate forms.

ACKNOWLEDGMENT

This work was supported by NSF YIA Grant No. DMR-9458005.

REFERENCES

- [1] J.M. Tatibouët and J.E. Germain, *J. Catal.*, **72**, 275 (1981).
- [2] U. Chowdhry, A. Ferretti, L.E. Firment, C.J. Machiels, F. Ohuchi, A.W. Sleight and R.H. Staley, *Appl. Surf. Sci.*, **19**, 360 (1984).
- [3] J.C. Volta and J.M. Tatibouët, *J. Catal.*, **93**, 467 (1985).
- [4] K. Bruckman, R. Grabowski, J. Haber, A. Mazurkiewicz, J. Sloczynski, and T. Wiltowski, *J. Catal.*, **104**, 71 (1987).
- [5] R.L. Smith and G.S. Rohrer, *J. Catal.*, **163**, 12 (1996).
- [6] R.L. Smith and G.S. Rohrer, *J. Solid State Chem.*, **124**, 104 (1996).
- [7] J.J. Birtill and P.G. Dickens, *Mat. Res. Bul.*, **13**, 311 (1978).
- [8] P. Vergnon and J.M. Tatibouët, *Bull. Soc. Chim. Fr.*, **11-12**, 455 (1980).
- [9] J. Guidot and J.E. Germain, *React. Kinet. Catal. Lett.*, **15**, 389 (1980).
- [10] R.L. Smith and G.S. Rohrer, *J. Catal.*, in press.
- [11] L.A. Bursill, *Proc. Roy. Soc.*, **A311**, 267 (1969).
- [12] L.A. Bursill, W.C.T. Dowell, P. Goodman, and N. Tate, *Acta Cryst.*, **A34**, 296 (1974).
- [13] P.L. Gai, *Phil. Mag. A*, **43**, 841 (1981).
- [14] P.L. Gai-Boyes, *Catal. Rev.-Sci. Eng.*, **34**, 1 (1992).
- [15] W.E. Farneth, F. Ohuchi, R.H. Staley, U. Chowdhry, and A.W. Sleight, *J. Phys. Chem.*, **89**, 2493 (1985).
- [16] C.J. Machiels and A.W. Sleight in Proceedings of the 4th International Conference on the Chemistry and Uses of Molybdenum (H.F. Barry and P.C.H. Mitchell, Eds.), p. 411. Climax Molybdenum Co., Ann Arbor, MI, 1982.